

GRAPHS WITH NONNEGATIVE RICCI CURVATURE AND MAXIMUM DEGREE AT MOST 3

FENGWEN HAN AND TAO WANG

ABSTRACT. In this paper, we classify graphs with nonnegative Lin-Lu-Yau-Ollivier Ricci curvature, maximum degree at most 3 and diameter at least 6.

1. INTRODUCTION

Ricci curvature is one of the most important geometric quantities in Riemannian geometry. For discrete settings, various definitions of Ricci curvature were developed over the past few decades. In this paper, we focus on Ollivier Ricci curvature and its variations. The original Ollivier Ricci curvature was developed on metric spaces and Markov chains, which can be applied on normalized graphs; see [Oll09, Oll07]. In 2011, Lin-Lu-Yau [LLY11] modified Ollivier's definition. This version was widely used in the research of normalized graphs. Münch and Wojciechowski [MW19] extended Lin-Lu-Yau's definition to general weighted graphs. Bakry-Émery curvature is another important Ricci curvature on graphs, readers may refer to [Sch99, LY10] for more details.

There are significant geometric and analytic results for Riemannian manifolds with nonnegative Ricci curvature. As discrete analogs, graphs with nonnegative Ricci curvature are also worthy to study. A basic method is to explore their local geometric structures. Many papers on this subject were published recently. Cushing et al. [CKL⁺19] classified all 3-regular graphs with nonnegative Bakry-Émery curvature. They also classified all 3-regular graphs with nonnegative original Ollivier Ricci curvature. Under the setting of Lin-Lu-Yau-Ollivier Ricci curvature, there are many works on the classification of Ricci-flat graphs, i.e. graphs whose Ricci curvature vanishes on every edge; see [CKL⁺18, LLY14, CP18, HLYY18, BLY21].

It is interesting to study harmonic functions on graphs. For the continuous case, Yau [Yau75] showed that positive harmonic functions on a complete, noncompact Riemannian manifold with nonnegative Ricci curvature are constant, which is known as Liouville property of harmonic functions. For the discrete case, there are also some known results. Jost, Münch and Rose [JMR19] proved that bounded harmonic functions are constant under the nonnegative Lin-Lu-Yau-Ollivier Ricci curvature condition. We also refer to [Hua19, BHL⁺15, HLLY19] for Liouville properties under the other curvature conditions. However, the strong Liouville property of graphs with

non-negative Lin-Lu-Yau-Ollivier Ricci curvature is still unknown. As an application of the main results, we prove that it is true for those graphs with maximum degree at most three.

Let \mathcal{G} be the class of combinatorial graphs with following properties:

1) Lin-Lu-Yau-Ollivier Ricci curvatures on all edges of $G \in \mathcal{G}$ are nonnegative;

2) Degrees of all vertices of $G \in \mathcal{G}$ are at most 3;

3) Diameters of the graphs in \mathcal{G} are at least 6.

The precise definition of \mathcal{G} is given in section 2. We classify all graphs in \mathcal{G} by the following two theorems.

Theorem 1.1. *Let $G \in \mathcal{G}$ be a finite graph. Then G is isomorphic to a finite path, a simple cycle, a prism graph, a Möbius ladder, a particular graph as shown in Figure 1, or a quasi-ladder graph as shown in Figure 2.*

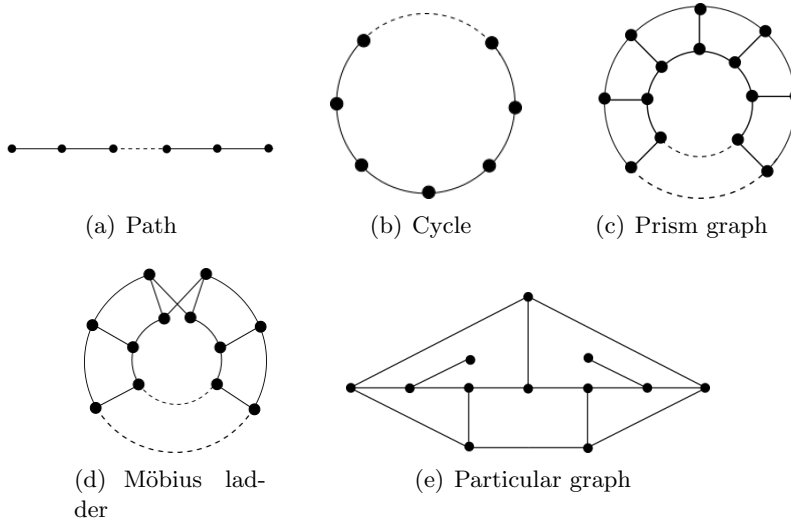


FIGURE 1

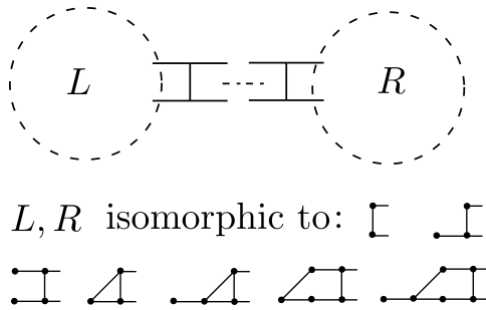


FIGURE 2. Quasi-ladder

Theorem 1.2. *Let $G \in \mathcal{G}$ be an infinite graph. Then G is isomorphic to one of the following graphs.*

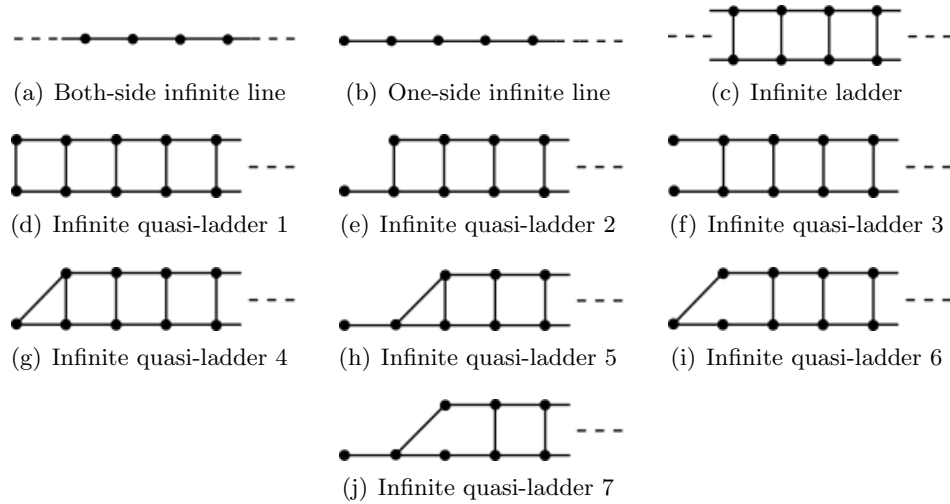


FIGURE 3

Remark 1.3. (1) *Theorem 1.1 and Theorem 1.2 also hold for normalized graphs; see Theorem 2.5.*
(2) *For normalized graphs, if we change the nonnegative Lin-Lu-Yau-Ollivier Ricci curvature constraint to nonnegative Ollivier Ricci curvature, we also get a classification; see Theorem 2.6.*
(3) *It is well known that manifolds with nonnegative Ricci curvature satisfy Cheeger-Gromoll splitting theorem [CG72]. As a discrete analog, the splitting theorem also holds for Graphs in \mathcal{G} , i.e. if a both-side infinite line is contained in $G \in \mathcal{G}$, then G is the Cartesian product of a line and a graph.*

Bai, Lu and Yau [BLY21] classified all Ricci-flat graphs with maximum degree at most 4. Compared with our results, they require a more stringent curvature condition but relax the maximum degree condition from 3 to 4, which causes a huge increase in the complexity of the problem.

The proofs of the main results are shown in section 4. We give a sketch here. Let $P = v_0 v_1 \cdots v_l$ be a diameter of $G \in \mathcal{G}$ with $l \geq 6$. The local structure along P can be characterized in Lemma 3.1, Lemma 3.3 and Lemma 3.4. Moreover, the subgraph induced by P and its neighbors is a quasi-ladder. We divide G into four parts as shown in Figure 4. If L is connected to R via O , we will get a special cycle (we call it a geodesic cycle in this paper) by Lemma 4.1, and we prove G has to be a cycle, a prism or a Möbius ladder by Lemma 4.2. If L is not connected to R via O , then $O = \emptyset$ and G is a quasi-ladder, otherwise we will find a longer geodesic path.

For infinite graphs, the proof is similar. For graphs with small diameter, say $l = 4$ or 5 , the structures are more complicated. However, since the maximum degree is at most 3, graphs with nonnegative curvature and small diameter can be enumerated by computers, which we are not going to explore in this paper.

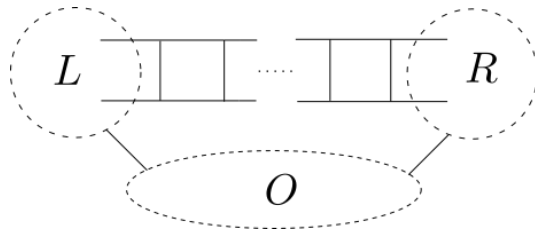


FIGURE 4

The paper is organized as follows: In next section, we introduce some notions on graphs and the definition of Ricci curvature. Section 3 gives the local structures of graph along a diameter, which serve as basic tools in the following discussions. In section 4, we prove the main results of this paper. In section 5, as an applications of the main results, we show that all positive harmonic functions on $G \in \mathcal{G}$ are constant.

2. PRELIMINARIES

2.1. Basic notions. Throughout this paper, we always assume that $G(V, E)$ is an undirected, connected, locally finite, simple graph with vertex set V and edge set E . Let $|G| := |V|$ be the number of vertices of the graph. For any vertices $u, v \in V$, we call v a *neighbor* of u if $\{u, v\} \in E$, denoted by $u \sim v$. For notational simplicity, we write uv for the unordered pair $\{u, v\}$. For $A, B \subset V$, let $E(A, B) := \{uv \in E : u \in A, v \in B\}$. The *degree* of a vertex $v \in V$ is defined via $\deg(v) := \#\{u \in V : u \sim v\}$. A graph $H(V', E')$ is called a *subgraph* of $G(V, E)$ if $V' \subseteq V$ and $E' \subseteq E$. A subgraph H is called an *induced subgraph* of G if $E' = \{\{u, v\} \in E : u, v \in V'\}$, and is denoted by $G(V')$. For $A, B \subseteq V'$, let $d_H(A, B) := \inf\{n : A \ni v_0 \sim \dots \sim v_n \in B\}$ be the *combinatorial distance* between A and B in subgraph $H(V', E')$. If $H = G$, we omit the subscript, i.e. $d(A, B) := d_G(A, B)$. If $A = \{u\}$ or $B = \{v\}$ is a single vertex subset, we will omit the braces, i.e. $d_H(u, v) := d_H(\{u\}, \{v\})$.

A *walk* W of length l is a sequence of vertices v_0, v_1, \dots, v_l such that $v_i \sim v_{i+1}$ for $i = 0, 1, \dots, l-1$. We write $W = v_0v_1 \dots v_l$ for short. If $v_0 = v_l$, we call it a *closed walk*. Moreover, a closed walk $W = v_0v_1 \dots v_l$ is called a *cycle* if $v_i \neq v_j$ for all $1 \leq i, j \leq l$. We also regard a cycle $C = v_0v_1 \dots v_l$ as a subgraph with vertex set $V(C) = \{v_0, v_1 \dots v_{l-1}\}$ and edge set $E(C) = \{\{v_i, v_{i+1}\} : i = 0, 1, \dots, l-1\}$. A walk $W = v_0v_1 \dots v_l$ is called a *path* if $v_i \neq v_j$ for all $0 \leq i, j \leq l$. We also regard a path $P = v_0v_1 \dots v_l$ as a subgraph with vertex set $V(P) = \{v_0, v_1 \dots v_l\}$ and edge set $E(P) = \{\{v_i, v_{i+1}\} : i = 0, 1, \dots, l-1\}$.

Let H be a subgraph of G . We say a path $P = v_0v_1 \cdots v_l$ is *geodesic* in H if $d_H(v_0, v_l) = l$. It is easy to know that $P = v_0v_1 \cdots v_l$ is a geodesic path of H if and only if $d_H(v_i, v_j) = |i - j|$ for all $0 \leq i, j \leq l$. We say H is a *geodesic subgraph* if all geodesic paths in H are also geodesic paths in G . It is not hard to verify that H is a geodesic subgraph of G if and only if $d_H(u, v) = d_G(u, v)$ for all $u, v \in H$. A *diameter path* of G is a longest geodesic path P in G . We let $\text{diam}(G)$ denote the length of a diameter path in G , i.e. $\text{diam}(G) = \sup\{d(u, v) : u, v \in V\}$.

A graph $G(V, E)$ is called *rooted at p* if a vertex $p \in V$ is specially appointed, denoted by (G, p) . We define $r : V \rightarrow \mathbb{N}^0$ via $r(u) = d(p, u)$. If $r(u) > 0$, there always exists a $v \sim u$ such that $r(v) = r(u) - 1$ and a geodesic path $p \cdots vu$ with length equals to $r(u)$. Given a geodesic path $P = v_0v_1 \cdots v_l$ in G , we always regard G as a graph rooted at v_0 if not specified.

Let $G(V, E)$ be a graph with degree at most 3, $P = v_0v_1 \cdots v_l$ be a geodesic path. For all $1 \leq i \leq l - 1$, v_i has at most one extra neighbor as v_{i-1} and v_{i+1} are two neighbors of v_i . We define a *state function* $s : \{v_i : 1 \leq i \leq l - 1\} \rightarrow \{2, 3^-, 3^0, 3^+\}$ via

$$s(v_i) = \begin{cases} 2, & \text{if } \deg(v_i) = 2, \\ 3^-, & \text{if } v_i \text{ has an extra neighbor } u_i \text{ and } r(u_i) < r(v_i), \\ 3^0, & \text{if } v_i \text{ has an extra neighbor } u_i \text{ and } r(u_i) = r(v_i), \\ 3^+, & \text{if } v_i \text{ has an extra neighbor } u_i \text{ and } r(u_i) > r(v_i). \end{cases}$$

As figures are quite important in the discussions of this paper, we explain the drawing style here. If not specified, a horizontal segment with vertices represents a geodesic path as shown in (a) of the following figure. If v_i has an extra neighbor u_i and $r(u_i) < r(v_i)$, i.e. $s(v_i) = 3^-$, we draw the figure as shown in (b) such that u_i has the same abscissa with v_{i-1} as $r(u_i) = r(v_{i-1})$. Figure (c) and (d) show the drawings when $r(u_i) = r(v_i)$ and $r(u_i) > r(v_i)$ respectively.

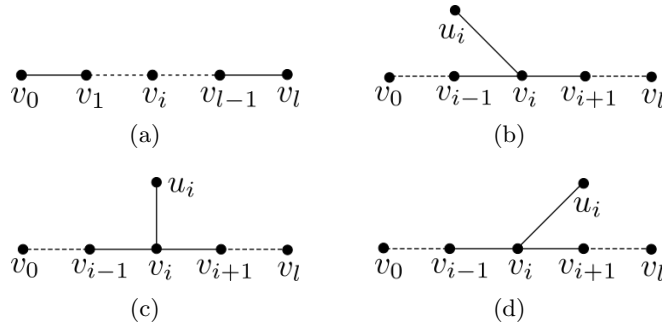


FIGURE 5

2.2. Ricci curvature on weighted graphs. Let

$$w : E \rightarrow (0, \infty), \{x, y\} \mapsto w(x, y) = w(y, x)$$

be the *edge weight* function,

$$m : V \rightarrow (0, \infty), x \mapsto m(x)$$

be the *vertex weight* function. We call the quadruple $G = (V, E, m, w)$ a *weighted graph*. Unless otherwise specified, we always regard a graph $G(V, E)$ as a *combinatorial graph*, i.e. $w \equiv 1$ and $m \equiv 1$. Our results also hold for *normalized graphs*, i.e. $w \equiv 1$ and $m(u) = \deg(u)$ for all $u \in V$; see Theorem 2.5.

We define the *Laplacian* $\Delta : \mathbb{R}^V \rightarrow \mathbb{R}^V$ via

$$\Delta f(u) := \frac{1}{m(u)} \sum_{v \sim u} w(u, v)(f(v) - f(u)).$$

A function f on G is called *harmonic* if $\Delta f \equiv 0$.

For a weighted graph $G(V, E, w, m)$, let $\text{Deg}(u) := \sum_{v \sim u} \frac{w(u, v)}{m(u)}$. We define a probability measure

$$\mu_u^\varepsilon(v) = \begin{cases} 1 - \varepsilon \text{Deg}(u) & : v = u; \\ \varepsilon w(u, v)/m(u) & : \text{otherwise.} \end{cases}$$

Particularly, for combinatorial graphs, we have

$$\mu_u^\varepsilon(v) = \begin{cases} 1 - \varepsilon \deg(u) & : v = u; \\ \varepsilon & : \text{otherwise.} \end{cases}$$

For normalized graphs, we have

$$\mu_u^\varepsilon(v) = \begin{cases} 1 - \varepsilon & : v = u; \\ \varepsilon / \deg(u) & : \text{otherwise.} \end{cases}$$

Definition 2.1. (*Wasserstein distance*) Let $G(V, E)$ be a graph, μ and ν be two probability measures on G . The Wasserstein distance $W(\mu, \nu)$ is given by

$$W(\mu, \nu) := \inf_A \sum_{u, v \in V} A(u, v) d(u, v),$$

where A is a coupling between μ and ν , i.e. a mapping $A : V \times V \rightarrow [0, 1]$ s.t.

$$\sum_{v \in V} A(u, v) = \mu(u) \text{ and } \sum_{u \in V} A(u, v) = \nu(v).$$

Definition 2.2. For any vertices $u, v \in G(V, E, w, m)$, the ε -Ollivier-Ricci curvature $\kappa_\varepsilon(u, v)$ is defined via

$$\kappa_\varepsilon(u, v) := 1 - \frac{W(\mu_u^\varepsilon, \mu_v^\varepsilon)}{d(u, v)}.$$

Specifically, the Ollivier Ricci curvature on a normalized graph is defined via

$$\kappa^O(u, v) := \kappa_1(u, v).$$

The Lin-Lu-Yau-Ollivier Ricci curvature $\kappa(u, v)$ is defined via

$$\kappa(u, v) := \lim_{\varepsilon \rightarrow 0^+} \frac{1}{\varepsilon} \kappa_\varepsilon(u, v).$$

For fixed vertices $u, v \in E$, it was shown in [BCL⁺18] that the function $\varepsilon \mapsto \kappa_\varepsilon(u, v)$ is concave and piecewise linear, so the limitation exists and κ is well defined. There are also equivalent limit-free definitions via coupling function or Laplacian on graphs; see [BHLY20, MW19]. When we say Ricci curvature or curvature in the following, we always mean the Lin-Lu-Yau-Ollivier Ricci curvature defined above.

For combinatorial graphs, Münch and Wojciechowski [MW19, Theorem 2.6] gave an easier way to calculate Ricci curvatures on edges as shown in the following theorem.

Theorem 2.3. *(Transport and combinatorial graphs) Let $G = (V, E)$ be a combinatorial graph and let $u \sim v$ be adjacent vertices. Let $B_{uv} := B_1(u) \cap B_1(v)$, $B_u^v := B_1(u) \setminus B_1(v)$ and $B_v^u := B_1(v) \setminus B_1(u)$. Let $\Phi_{uv} := \{\phi : D(\phi) \subseteq B_u^v \rightarrow R(\phi) \subseteq B_v^u : \phi \text{ bijective}\}$. For $\phi \in \Phi_{uv}$ write $D(\phi)^c := B_u^v \setminus D(\phi)$ and $R(\phi)^c := B_v^u \setminus R(\phi)$. Then*

$$\kappa(u, v) = \#B_{uv} - \inf_{\phi \in \Phi_{uv}} \left(\#D(\phi)^c + \#R(\phi)^c + \sum_{w \in D(\phi)} [d(w, \phi(w)) - 1] \right).$$

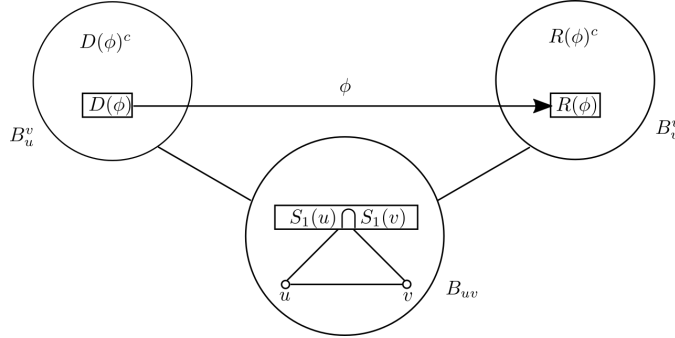


FIGURE 6

We always suppose $\#D(\phi)^c = 0$ or $\#R(\phi)^c = 0$ when applying Theorem 2.3. If ϕ is an optimal map such that $u \in D(\phi)^c$ and $v \in R(\phi)^c$, we extend ϕ by adding an extra map $\phi(u) = v$. It is easy to verify that the new ϕ is still an optimal map. So our hypothesis is fair. The following is a direct corollary of Theorem 2.3.

Corollary 2.4. *Let $G = (V, E)$ be a combinatorial graph and let $u \sim v$ be adjacent vertices. Let $N_w := B_1(w) \setminus \{u, v\}$ be the set of extra neighbors of w , $w \in \{u, v\}$. If $|N_u| + |N_v| \geq 3$ and $d(N_u, N_v) \geq 3$, we have $\kappa(u, v) < 0$.*

Let $\kappa(G) := \inf_{\{u,v\} \in E} \kappa(u, v)$ be the Ricci curvature of G and $\deg(G) := \sup_{u \in V} \deg(u)$ the maximum degree of G . The class of graphs we will classify in this paper is defined by

$$\mathcal{G} := \{G(V, E) : \deg(G) \leq 3, \kappa(G) \geq 0, \text{diam}(G) \geq 6\}.$$

Cushing et al. [CKL⁺19] provide a powerful online tool, the Graph Curvature Calculator, to calculate various of curvatures on graphs. Readers can find it on <https://www.mas.ncl.ac.uk/graph-curvature/>. By using this tool, it is convenient to check that the Ricci curvatures of graphs in Figure 1, 2 and 3 are nonnegative. We also use it to prove the following theorems.

Theorem 2.5. *Let $G = (V, E)$ be a graph with $\deg(G) \leq 3$. Let G_C be the combinatorial graph and G_N be the normalized graph obtained by equipping G with combinatorial weight and normalized weight respectively. Then $\kappa(G_C) \geq 0$ if and only if $\kappa(G_N) \geq 0$.*

Proof. For any $uv \in E$, let $\kappa_C(uv)$ be the curvature of uv when G is equipped with combinatorial weight and $\kappa_N(uv)$ be the curvature of uv when G is equipped with normalized weight. If $\deg(u) = 1$ or $\deg(v) = 1$, we have $\kappa_C(uv) \geq 0$ and $\kappa_N(uv) \geq 0$ by a direct calculation. If $\deg(u) = \deg(v)$, we have $\kappa_C(uv) = \deg(u) \cdot \kappa_N(uv)$ by the definition of Ricci curvature. So we only need to consider the case that $\deg(u) = 2$ and $\deg(v) = 3$, i.e. u has an extra neighbor u' , v has two extra neighbors v' and v'' . Then $\kappa_C(uv)$ and $\kappa_N(uv)$ depend only on the distances $d(u', v')$ and $d(u', v'')$. By a direct calculation, we have $\kappa_C(uv) < 0 \Leftrightarrow d(u', v') = d(u', v'') = 3 \Leftrightarrow \kappa_N(uv) < 0$. This completes the proof. \square

It is noteworthy that Theorem 2.5 does not hold for graphs with maximum degree larger than 3. The minimum Ricci curvatures of the following graphs are 0, 0.5, -0.133 as normalized graphs and -1, -1, 0 as combinatorial graphs respectively.¹

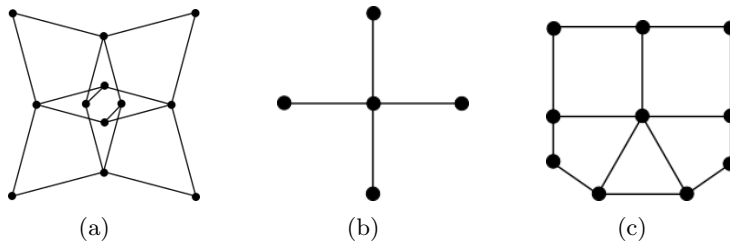


FIGURE 7

¹Graph (a) built by Bai-Lu-Yau [BLY21] is Ricci-flat as a normalized graph. Graphs (b) and (c) are pointed out to us by Florentin Münch.

Theorem 2.6. *Let G be a normalized graph with nonnegative Ollivier Ricci curvature, maximum degree at most 3 and diameter at least 6. If G is finite, then it is isometric to a finite path, a simple cycle, a prism graph, a Möbius ladder or a quasi-ladder as shown in the following figure. If G is infinite, then it is isometric to (a), (b), (c), (d), (e), (f), (g) or (h) of Figure 3.*

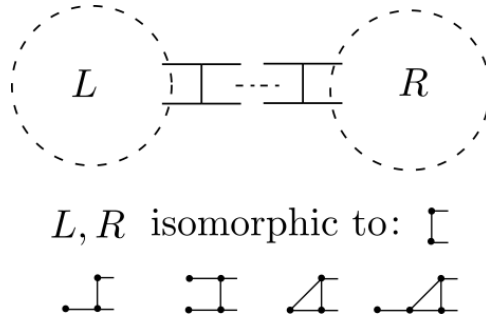


FIGURE 8. Quasi-ladder

Proof. For normalized graphs, $\kappa_0(u, v) \equiv 0$ for all $u, v \in V$. If $\kappa^O(u, v) \geq 0$, we always have $\kappa(u, v) \geq 0$, as the function $\varepsilon \mapsto \kappa_\varepsilon(u, v)$ is concave and piecewise linear; see [BCL⁺18, Theorem 1.1]. This indicates that all normalized graphs with nonnegative Ollivier Ricci curvature are also graphs with nonnegative Lin-Lu-Yau-Ollivier Ricci curvature. We check the Ollivier Ricci curvatures of graphs in Figure 1, 2, 3 by using the Graph Curvature Calculator and get the result. \square

3. THE LOCAL STRUCTURES

In this section, we study the local structure on a geodesic path of a graph $G \in \mathcal{G}$.

Lemma 3.1. *Let $P = v_0 \cdots v_i v_{i+1} v_{i+2} v_{i+3} \cdots v_l$ be a geodesic path of $G \in \mathcal{G}$.*

Case (2, 2): If $(s(v_{i+1}), s(v_{i+2})) = (2, 2)$, then G contains the following as a subgraph.

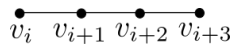


FIGURE 9. Case (2, 2)

Case (2, 3⁻): If $(s(v_{i+1}), s(v_{i+2})) = (2, 3^-)$, then G contains one of the followings as a subgraph.

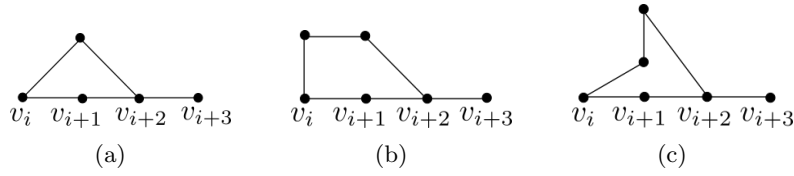


FIGURE 10. Case $(2, 3^-)$

Case $(2, 3^0)$: If $(s(v_{i+1}), s(v_{i+2})) = (2, 3^0)$, then G contains the following as a subgraph.

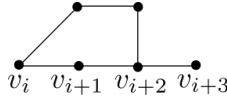


FIGURE 11. Case $(2, 3^0)$

Case $(2, 3^+)$: The situation $(s(v_{i+1}), s(v_{i+2})) = (2, 3^+)$ can not exist.

Case $(3^-, 2)$: The situation $(s(v_{i+1}), s(v_{i+2})) = (3^-, 2)$ can not exist.

Case $(3^0, 2)$: If $(s(v_{i+1}), s(v_{i+2})) = (3^0, 2)$, then G contains the following as a subgraph.

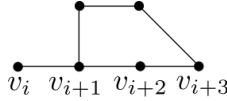


FIGURE 12. Case $(3^0, 2)$

Case $(3^+, 2)$: If $(s(v_{i+1}), s(v_{i+2})) = (3^+, 2)$, then G contains one of the followings as a subgraph.

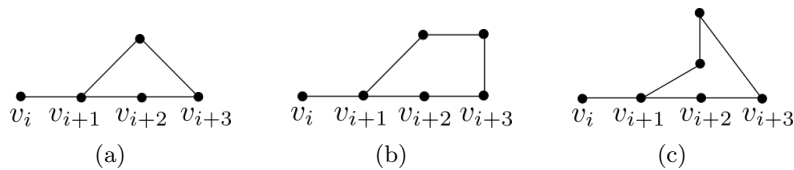


FIGURE 13. Case $(3^+, 2)$

Case $(3^-, 3^-)$: If $(s(v_{i+1}), s(v_{i+2})) = (3^-, 3^-)$, then G contains one of the followings as a subgraph.

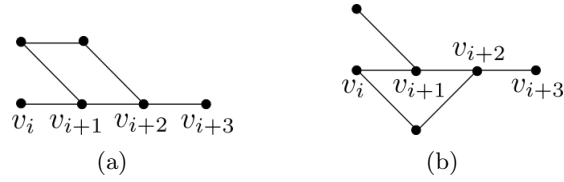


FIGURE 14. Case $(3^-, 3^-)$

Case $(3^-, 3^0)$: The situation $(s(v_{i+1}), s(v_{i+2})) = (3^-, 3^0)$ can not exist.

Case $(3^-, 3^+)$: The situation $(s(v_{i+1}), s(v_{i+2})) = (3^-, 3^+)$ can not exist.

Case $(3^0, 3^-)$: If $(s(v_{i+1}), s(v_{i+2})) = (3^0, 3^-)$, then G contains one of the followings as a subgraph.

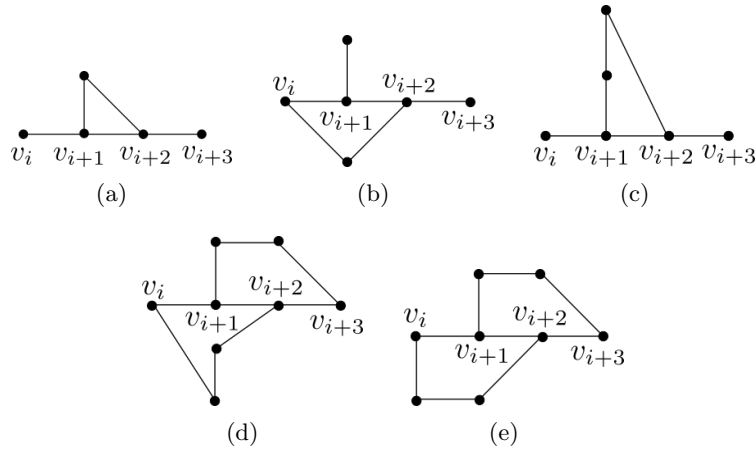


FIGURE 15. Case $(3^0, 3^-)$

Case $(3^0, 3^0)$: If $(s(v_{i+1}), s(v_{i+2})) = (3^0, 3^0)$, then G contains one of the followings as a subgraph.

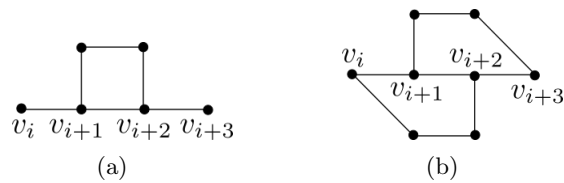


FIGURE 16. Case $(3^0, 3^0)$

Case $(3^0, 3^+)$: The situation $(s(v_{i+1}), s(v_{i+2})) = (3^0, 3^+)$ can not exist.

Case $(3^+, 3^-)$: If $(s(v_{i+1}), s(v_{i+2})) = (3^+, 3^-)$, then G contains one of the followings as a subgraph.

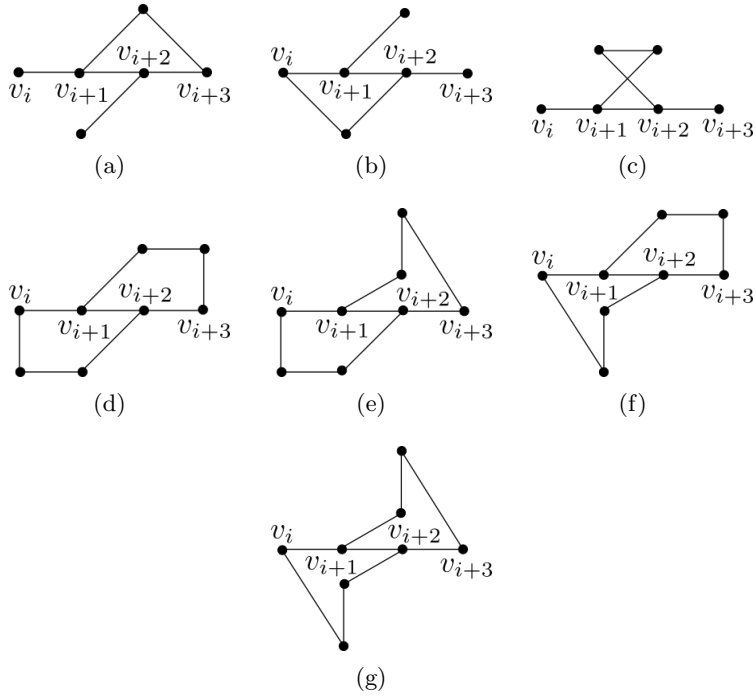


FIGURE 17. Case $(3^+, 3^-)$

Case $(3^+, 3^0)$: If $(s(v_{i+1}), s(v_{i+2})) = (3^+, 3^0)$, then G contains one of the followings as a subgraph.

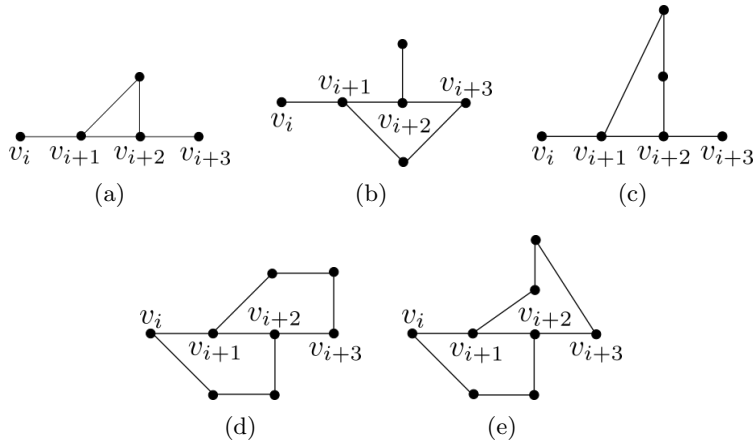


FIGURE 18. Case $(3^+, 3^0)$

Case $(3^+, 3^+)$: If $(s(v_{i+1}), s(v_{i+2})) = (3^+, 3^+)$, then G contains one of the followings as a subgraph.

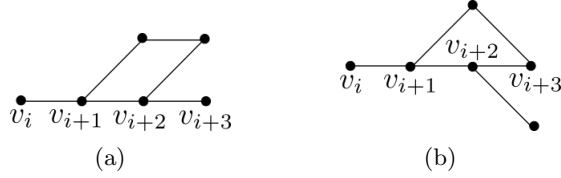


FIGURE 19. Case $(3^+, 3^+)$

Proof. We only show the proof of case $(2, 3^-)$, proofs for other cases are similar. Without loss of generality, let $i = 0$. Then G has a subgraph as shown in the following figure with $\deg(v_1) = 2$.

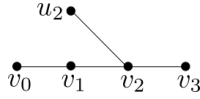


FIGURE 20

By Theorem 2.3 we have

$$\kappa(v_1, v_2) = \#B_{v_1v_2} - \inf_{\phi \in \Phi_{v_1v_2}} (\#D(\phi)^c + \#R(\phi)^c + \sum_{w \in D(\phi)} [d(w, \phi(w)) - 1]),$$

where $B_{v_1v_2} = \{v_1, v_2\}$, $\Phi_{v_1v_2} = \{\text{all maps from } \{v_0\} \text{ to } \{v_3, u_2\}\}$, $\#D(\phi)^c = 0$, and $\#R(\phi)^c = 1$. Then we have

$$\begin{aligned} 0 &\leq \kappa(v_1, v_2) \\ &= 2 - \inf_{\phi(v_0) \in \{v_3, u_2\}} (0 + 1 + d(v_0, \phi(v_0)) - 1) \\ &= \max\{2 - d(v_0, v_3), 2 - d(v_0, u_2)\}. \end{aligned}$$

As $d(v_0, v_3) = 3$, we have $d(v_0, u_2) = 1$ or $d(v_0, u_2) = 2$. If $d(v_0, u_2) = 1$, G contain (a) of Figure 10 as a subgraph. If $d(v_0, u_2) = 2$, G contains (b) or (c) of Figure 10 as a subgraph. This completes the proof. \square

By applying case $(\cdot, 3^+)$ or case $(3^-, \cdot)$ of Lemma 3.1 repeatedly, we get the following corollary.

Corollary 3.2. *Let $P = v_0v_1 \cdots v_l$ be a geodesic path in $G \in \mathcal{G}$, $l \geq 4$.*

1) *If there exists a $i \in \{1, 2, \dots, l-1\}$ such that $s(v_i) = 3^+$, then $s(v_j) = 3^+$ for all $1 \leq j \leq i$ and G has a subgraph (b) or (c) of the following figure.*

2) *If there exists a $i \in \{2, \dots, l-1\}$ such that $s(v_i) = 3^-$, then $s(v_j) = 3^-$ for all $i \leq j \leq l-1$ and G has a subgraph (e) or (f) of the following figure.*

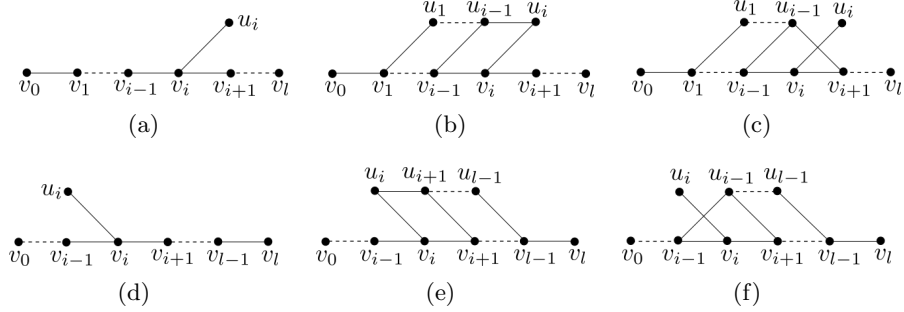


FIGURE 21

As a supplement to Lemma 3.1, we explore the local structures on long geodesic paths in the following two lemmas,

Lemma 3.3. *Let $P = v_0 \cdots v_i v_{i+1} v_{i+2} v_{i+3} \cdots v_l$ be a geodesic path with $l \geq 6$. If G contains (b) of Figure 16 as a subgraph, then G is isometric to the particular graph (e) of Figure 1.*

Proof. If $i = 2$, G contains a subgraph (a) of the following figure. By Corollary 3.2, G contains a subgraph (b). By applying case $(3^+, 3^0)$ of Lemma 3.1 on $v_1 v_2 v_3 v_4$, G contains a subgraph (c). By applying case $(3^+, 3^0)$ of Lemma 3.1 on $v_1 u_1 u_3 u_5$, G contains a subgraph (d). Moreover, $\deg(v_0) = \deg(v_6) = 1$ by Corollary 2.4. So G is isometric to graph (d) of the following figure, which is isometric to (e) of Figure 1. If $i \neq 2$, it is impossible to get a graph with nonnegative Ricci curvature by a similar argument. This proves the lemma.

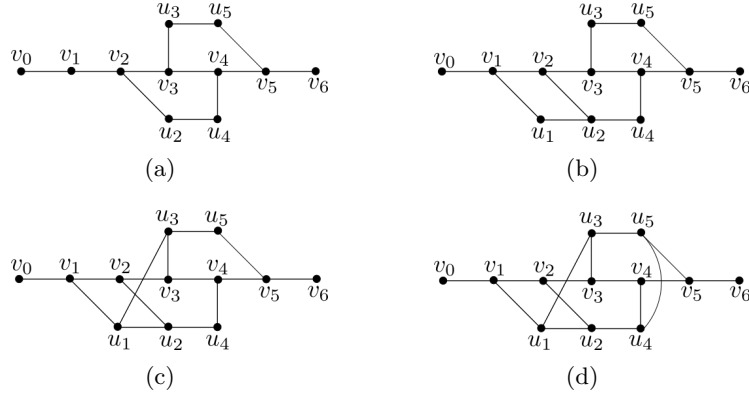


FIGURE 22

□

Lemma 3.4. *Let $P = v_0 \cdots v_i v_{i+1} v_{i+2} v_{i+3} \cdots v_l$ be a geodesic path with $l \geq 6$. Then none of the followings can be a subgraph of G : (c) in Figure*

10; (c) in Figure 13; (c), (d) and (e) in Figure 15; (c), (d), (e), (f) and (g) in Figure 17; (c), (d) and (e) in Figure 18.

Proof. We only show (c) of Figure 13 can not be a subgraph of G . Proofs for other cases are similar. We prove by contradiction. Suppose $i \leq 1$, then $i + 5 \leq l$ and G contains a subgraph (a) of the following figure with $\deg(v_{i+2}) = 2$ by Corollary 3.2. This is impossible as $\deg(u_{i+3}) \leq 3$ and u_{i+3} must have an extra neighbor w_{i+3} with $r(w_{i+3}) < r(u_{i+3})$. Suppose $2 \leq i \leq l - 4$. Then G contains a subgraph (b) of the following figure with $\deg(v_{i+2}) = 2$ by Corollary 3.2. Applying case $(3^0, 3^-)$ of Lemma 3.1 on $P' = v_0 \cdots w_{i+3} u_{i+3} v_{i+3} v_{i+4} \cdots$, we get a contradiction. Suppose $i = l - 3$. Then G contains a subgraph (c) of the following figure with $\deg(v_{l-1}) = 2$ by Corollary 3.2. We have $\kappa(u_l, u_{l-2}) < 0$ by Theorem 2.3. This completes the proof.

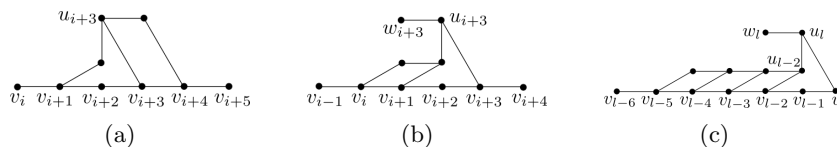


FIGURE 23

□

4. CLASSIFICATION OF GRAPHS

Let $G \in \mathcal{G}$ be a finite graph and $P = v_0 v_1 \cdots v_l$ be a diameter of G . Then P is a geodesic path. We explore all the available structures of G separately by the following four cases.

Case (i): For all $1 \leq i \leq l - 1$, $s(v_i) = 2$. We discuss this case in Theorem 4.3.

Case (ii): There exists a v_i such that $s(v_i) = 3^0$. We discuss this case in Theorem 4.5.

Case (iii): There exists a v_i such that $s(v_i) = 3^-$. We discuss this case in Theorem 4.6.

Case (iv): There exists a v_i such that $s(v_i) = 3^+$. We discuss this case in Theorem 4.7.

We firstly introduce two lemmas.

Lemma 4.1. *Let $G(V, E)$ be a finite graph. Suppose $V = A \sqcup B \sqcup C_1 \sqcup C_2$ satisfying:*

- (1) $E(A, B) = E(C_1, C_2) = \emptyset$;
- (2) The induced subgraphs $G(C_1)$ and $G(C_2)$ are complete graphs, i.e. for all $u, v \in C_i$, $u \sim v$ in $G(C_i)$, $i = 1, 2$;
- (3) The induced subgraphs $G_A = G(A \sqcup C_1 \sqcup C_2)$ and $G_B = G(B \sqcup C_1 \sqcup C_2)$

are connected graphs.

Then G contains a geodesic cycle C with $|C| \geq d_{G_A}(C_1, C_2) + d_{G_B}(C_1, C_2)$.

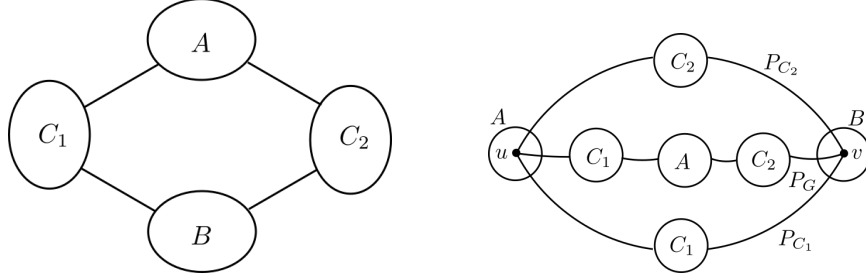


FIGURE 24

Proof. Let $\mathcal{C} = \{W \text{ is a closed walk} : W = P_1 P_A P_2 P_B, \text{ where } P_1, P_2, P_A \text{ and } P_B \text{ are walks in } C_1, C_2, A \text{ and } B \text{ respectively}\}$. Let $C \in \mathcal{C}$ with shortest length, then it is a cycle. Moreover, we can prove that C is a geodesic cycle. Suppose not, there are $u, v \in C$ such that $d_G(u, v) < d_C(u, v)$. We only prove the case that $u \in A$ and $v \in B$, proofs for other cases are similar.

Let P_G be a shortest walk between u and v in G and P_{C_i} be a shortest walk between u and v in C crossing C_i , $i = 1, 2$. Note that P_{C_1} and P_{C_2} are disjoint paths from u to v and C is the union of them.

Next, we claim that P_G has one of the following forms: $P_A P_1 P'_A P_2 P_B$, $P_A P_1 P_B P_2 P'_B$, $P_A P_2 P'_A P_1 P_B$, $P_A P_2 P_B P_1 P'_B$, $P_A P_1 P_B$ or $P_A P_2 P_B$. In fact, it is easy to see that $P_G \cap C_1$ is connected in P_G and $|P_G \cap C_1| \leq 2$ as C_1 is complete and P_G is a shortest walk. The same conclusion holds for $P_G \cap C_2$. So the claim holds.

Now, if $P_G = P_A P_1 P'_A P_2 P_B$, then P_G and P_{C_1} form a closed walk. By connecting C_1 part in P_G and C_1 part in P_{C_1} , we get a new closed walk $C' \in \mathcal{C}$ with a shorter length. This contradicts to the fact that C is a shortest walk. Proofs for other forms are similar. Then we proved $d_G(u, v) = d_C(u, v)$ for all $u, v \in C$, i.e. C is a geodesic cycle. The inequality $|C| \geq d_{G_A}(C_1, C_2) + d_{G_B}(C_1, C_2)$ is obtained directly from the construction of C . \square

Lemma 4.2. *Suppose $G \in \mathcal{G}$ contains a geodesic cycle C with $|C| \geq 8$, then $|C| \geq 11$ and G must be a cycle, a prism graph or a Möbius ladder.*

Proof. Suppose $|C| = 8$. We assume that there exists a vertex, say v_0 , has an extra neighbor u_0 , otherwise $G = C$. Note that every path P in C with $|P| \leq 5$ is geodesic in G .

We claim that G is a prism or Möbius ladder if $u_0 \sim v_2$. By applying local structure $(3^-, \cdot)$ on $v_1 v_2 v_3 v_4$ in (G, v_0) , we get that G contains (a) or (b) of the following figure as a subgraph. By symmetric, G has a subgraph (c) or (d) in the following figure. By doing this repeatedly, we get that G has a subgraph (e). Finally we get a prism graph or a Möbius ladder.

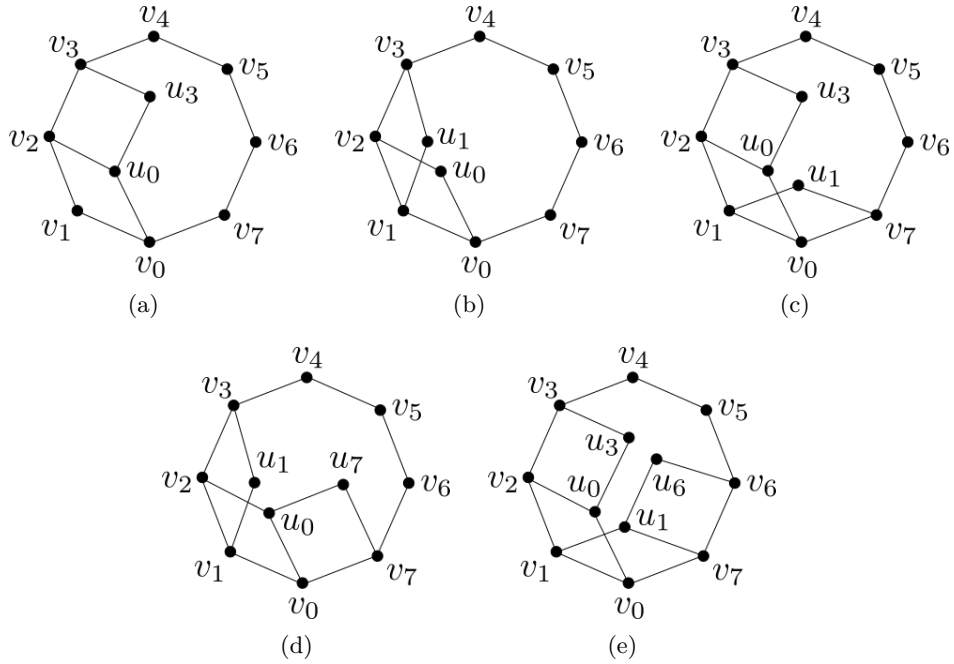


FIGURE 25

We claim that u_0 is not a neighbor of v_1 . Suppose not, G has a subgraph (a) of the following figure. Applying local structure $(3^0, \cdot)$ on $v_0v_1v_2v_3$ in (G, v_0) , we know that G has a subgraph (b) or (c) of the following figure. This is impossible by the symmetry of the geodesic cycle. So our claim is true.

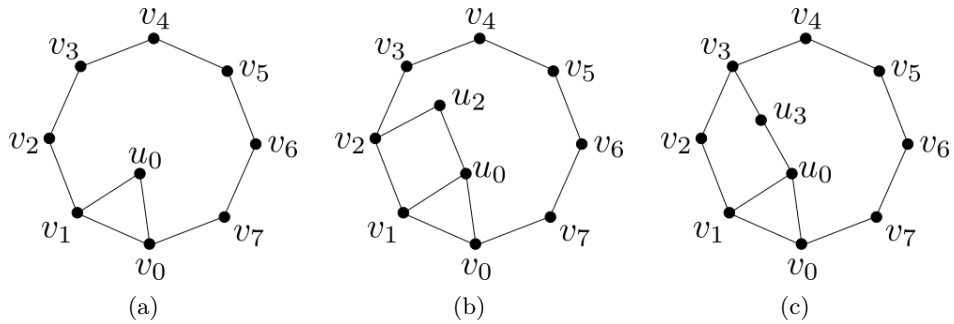


FIGURE 26

The previous claim also shows $u_0 \approx v_7$. By applying local structure $(3^+, \cdot)$ on $v_7v_0v_1v_2$ in (G, v_7) , we know that G has one of the following subgraphs.

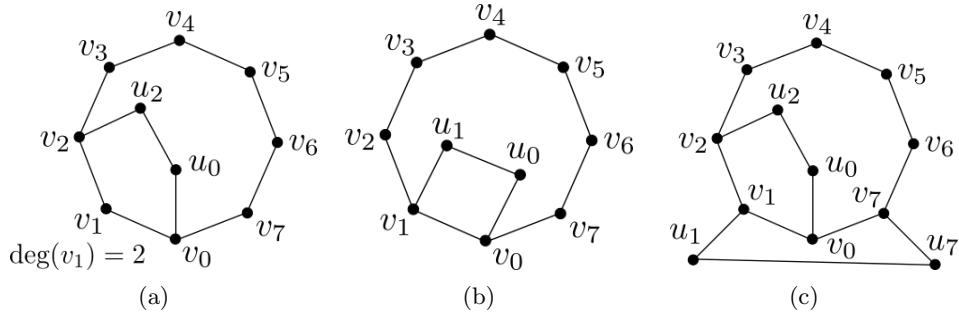


FIGURE 27

By applying local structures on C as we did previously, we get the following results. If G has a subgraph (c) in Figure 27, then G is isomorphic to (a) of Figure 28. Otherwise G must be isometric to (b), (c) or (d) of the following figure if G is not a prism graph or Möbius ladder.

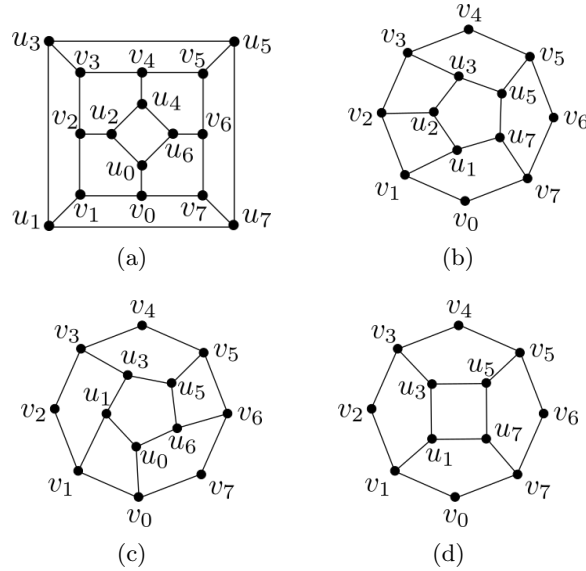


FIGURE 28

Note that the diameters of all the possible graphs we get are less than 6, thus they are not elements of \mathcal{G} . It follows that $|C| \neq 8$. We also have $|C| \neq 9, 10$ with similar arguments. When we do the previous steps on a geodesic cycle C with $|C| \geq 11$, the graphs with the same forms shown in Figure 28 contain edges with negative curvature. This indicates that G must be a cycle, prism graph or Möbius ladder.

□

Theorem 4.3. Let $P = v_0v_1 \cdots v_l$ be a diameter of $G \in \mathcal{G}$ with $l \geq 6$. If for all $1 \leq i \leq l-1$, $s(v_i) = 2$, then $G = P$ or isometric to a cycle.

Proof. Let $G_B := G(V \setminus \{v_0, v_1, \dots, v_l\})$. If v_0 is not connected to v_l via G_B , then $G = P$, otherwise we will get a longer diameter. If v_0 is connected to v_l via G_B . By setting $C_1 = \{v_0\}$ and $C_2 = \{v_l\}$ and applying Lemma 4.1, we get a geodesic cycle C with $|C| \geq 12$. Then the theorem holds by Lemma 4.2. \square

Lemma 4.4. Let $P = v_0v_1 \cdots v_l$, $l \geq 6$ be a diameter of $G \in \mathcal{G}$. If there exists $3 \leq i \leq l-3$ such that $s(v_i) = 3^0$, then $s(v_j) = 3^0$ for all $3 \leq i \leq l-3$, and G contains a subgraph shown in the following figure.

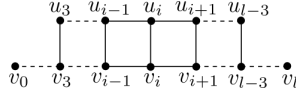


FIGURE 29

Proof. If $l = 6$, it is trivial. Suppose $l \geq 7$ and $i+1 \leq l-3$.

Firstly we prove $s(v_{i+1}) = 3^0$. If $s(v_{i+1}) = 2$, by applying local structure $(3^0, 2)$ on $v_{i-1}v_iv_{i+1}v_{i+2}$ and Corollary 3.2, we know that G contains the following figure as a subgraph with $\deg(v_{i+1}) = 2$. As $r(u_i) > 0$, there is a vertex $w_i \sim u_i$ with $r(w_i) < r(u_i)$. By applying local structure $(3^0, 3^+)$ on $w_iu_iu_{i+2}u_{i+3}$, we get a contradiction. If $s(v_{i+1}) = 3^-$, by applying local structure $(3^0, 3^-)$ on $v_{i-1}v_iv_{i+1}v_{i+2}$ and Corollary 3.2, we also get a contradiction. It follows that $s(v_{i+1}) = 3^0$. By applying local structure $(3^0, 3^0)$ on $v_{i-1}v_iv_{i+1}v_{i+2}$, we have $u_i \sim u_{i+1}$. If $i-1 \geq 3$, with the similar argument, we can also prove that $s(v_{i-1}) = 3^0$.

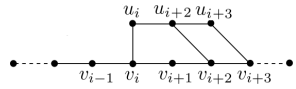


FIGURE 30

By taking the previous steps repeatedly, we complete the proof. \square

Theorem 4.5. Let $P = v_0v_1 \cdots v_l$, $l \geq 6$, be a diameter of $G \in \mathcal{G}$. If there exists a $i \in \{1, 2, \dots, l-1\}$ such that $s(v_i) = 3^0$, then G is a quasi-ladder or isometric to the particular graph (d) in Figure 1.

Proof. Let $k = \min\{i : s(v_i) = 3^0, 1 \leq i \leq l-1\}$. By Lemma 4.4, we have $k \in \{1, 2, 3, l-2, l-1\}$.

Case (i): $k = 1$. G contains (a) of the following figure as a subgraph. We claim that $s(v_j) = 3^0$ or 3^- for all $2 \leq j \leq l-3$. If $s(v_2) = 2$, by applying local structure $(3^0, 2)$ on $v_0v_1v_2v_3$, we have that G has a subgraph (b) of the following figure. By applying local structure $(3^0, 3^+)$ on $v_0u_0u_3u_4$, we

get a contradiction. If $s(v_2) = 3^+$, we also get a contradiction by applying $(3^0, 3^+)$ on $v_0v_1v_2v_3$. So $s(v_2) = 3^0$ or 3^- .

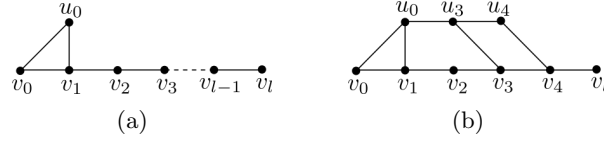


FIGURE 31

If $s(v_2) = 3^0$, we have $u_0 \sim u_2$ as shown in (a) of the following figure by applying local structure $(3^0, 3^0)$ on $v_0v_1v_2v_3$. The previous argument tells us that $s(v_3) \neq 2, 3^+$. It is not hard to verify that $s(v_3) \neq 3^-$ neither. So $s(v_3) = 3^0$ and $u_2 \sim u_3$. By Lemma 4.4, G has a subgraph (a) of the following figure. Moreover, $\deg(v_0) = 2$, otherwise v_0 has an extra neighbor w_0 . Then $\deg(w_0) = 1$ by Corollary 2.4 and $d_G(w_0, v_l) = l + 1$, which is contrary to $\text{diam}(G) = l$. If $s(v_2) = 3^-$, by Corollary 3.2 we have $s(v_i) = 3^-$ for $i \in \{2, 3, \dots, l-1\}$ and G has a subgraph (b) of the following figure. Moreover, $\deg_G(u_0) = 2$ and $u_0v_1v_2 \cdots v_l$ is also a diameter of G . We can redraw (b) as shown in (c) of the following figure, which contains (a) as a subgraph. So we only need to consider the situation that G contains a subgraph (a).

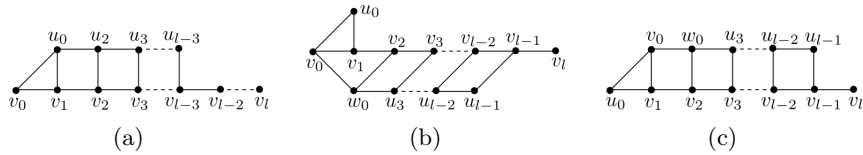


FIGURE 32

As we see, the left side of G is fixed, we start to study the structure of the right side. If $\deg(v_{l-2}) = 2$, G contains a subgraph (a) of the following figure by applying local structure $(3^0, 2)$ on $v_{l-4}v_{l-3}v_{l-2}v_{l-1}$. If $\deg(v_{l-2}) = 3$, we have $s(v_{l-2}) = 3^0$ and $u_{l-3} \sim u_{l-2}$. With similar arguments, we classify all possible structures of the right side of G as shown in the following figure.

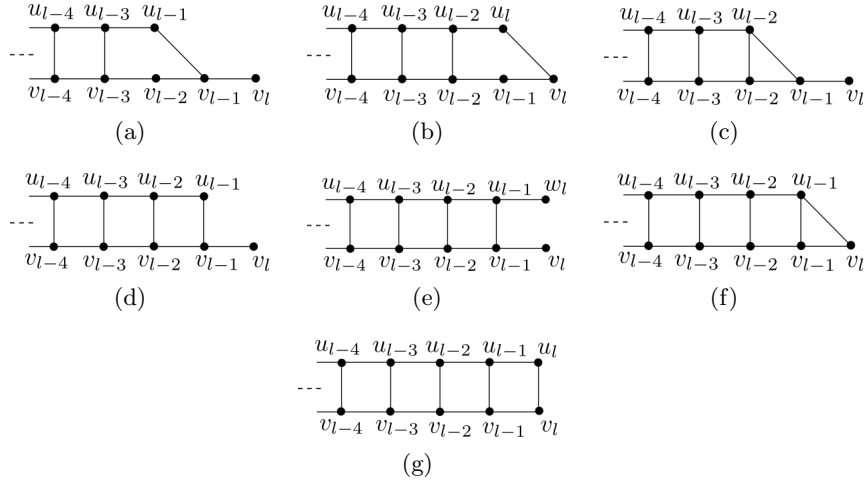


FIGURE 33

Case (ii): $k = 2$. By applying $(\cdot, 3^0)$ on $v_0v_1v_2v_3$, G contains a subgraph (a), (b) or (c) shown in the following figure. Obviously situation (c) is contained in (b) as $u_0u_2v_2v_3 \cdots$ in (c) is also a diameter. We only need to consider the situation that G has a subgraph (a) or (b). It is easy to verify that $\deg(v_0) = 1$ in (a) and $\deg(v_0) = \deg(v_1) = \deg(u_0) = 2$ in (b). So the left-hand side is fixed. The right-hand side of G is the same with that in case (i).

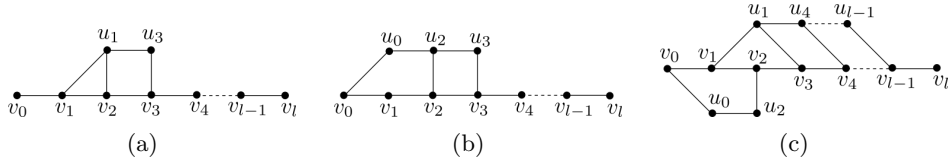


FIGURE 34

Case (iii): $k = 3$. If $l \geq 7$, the left side of G is shown as following. The available structures of the right side are the same with that in case (i). If $l = 6$, G has an additional available structure shown in (d) of Figure 1.

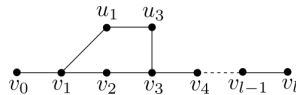


FIGURE 35

Case (iv): $k = l - 2$. It is easy to verify this case can not happen.

Case (v): $k = l - 1$. G has a subgraph (a) or (b) shown in the following figure. As $v_l v_{l-1} \cdots v_0$ is also a diameter, graphs in this case have been discussed in the previous cases.

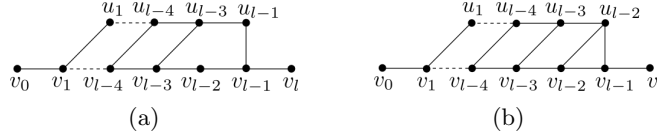


FIGURE 36

By previous discussions, we prove that G must be a quasi-ladder graph with the following structures or isometric to the particular graph (d) in Figure 1.

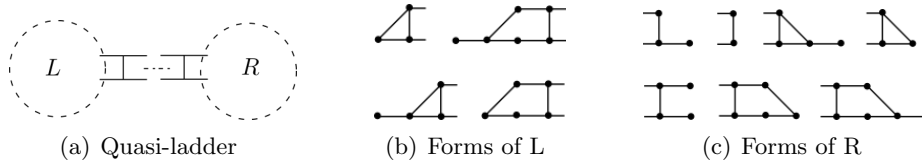


FIGURE 37

□

Theorem 4.6. Let $P = v_0 v_1 \cdots v_l$, $l \geq 6$, be a diameter of $G \in \mathcal{G}$. If for all $1 \leq i \leq l - 1$, $s(v_i) \neq 3^0$, and there exists v_i such that $s(v_i) = 3^-$, then G is a prism graph, a Möbius ladder or a quasi-ladder.

Proof. Let $k = \min\{i : 1 \leq i \leq l - 1, s(v_i) = 3^-\}$, then $k \geq 2$.

Case (i): If $k = 2$, G has a subgraph (a) of the following figure. By Corollary 3.2, G has a subgraph (b) or (c) of the following figure. By switching u_0 and v_1 in (b), we get (b) is the same with (c). So we only consider the case that G contains a subgraph (b).

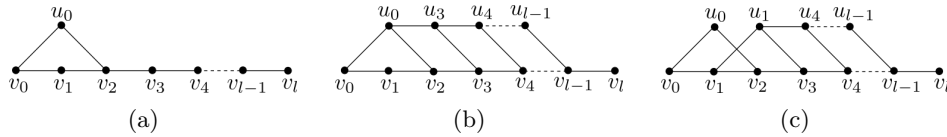


FIGURE 38

Let $C_1 = G(\{v_0, v_1\})$, $G_A = G(\{u_0, u_3, \dots, u_{l-2}, v_2, v_3 \cdots, v_{l-2}\})$, $C_2 = G(\{v_{l-1}, u_{l-1}\})$ and $G_B = G(V \setminus \{u_0, u_3, \dots, u_{l-1}, v_0, v_1 \cdots, v_l\})$. If C_1 is connected to C_2 via G_B , we get a geodesic cycle C with $|C| \geq 8$ by Lemma

4.1 and G must be a prism graph or Möbius ladder by Lemma 4.2. In the following, we suppose that C_1 is not connected to C_2 via G_B . With a similar argument in the proof of Theorem 4.5, the left side of G has one of the following forms.

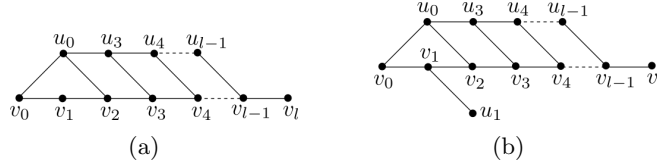


FIGURE 39

We start to deal with the right-hand side. If $\deg(u_{l-1}) = 2$, we have $\deg(v_l) = 1$ by Corollary 2.4 and the structure of the right-hand side is (a) of the following figure. If u_{l-1} has an extra neighbor w_{l-1} , we have $r(u_{l-1}) < r(w_{l-1})$. Otherwise, w_{l-1} has an extra neighbor w' and $\kappa(w', w_{l-1}) < 0$ by Corollary 2.4. If $\deg(w_{l-1}) = 1$, we have $\deg(v_l) = 1$ and the right-hand side structure is shown in (b) of the following figure. With similar arguments, we find all possible forms of the right side of G as shown in the following figure.

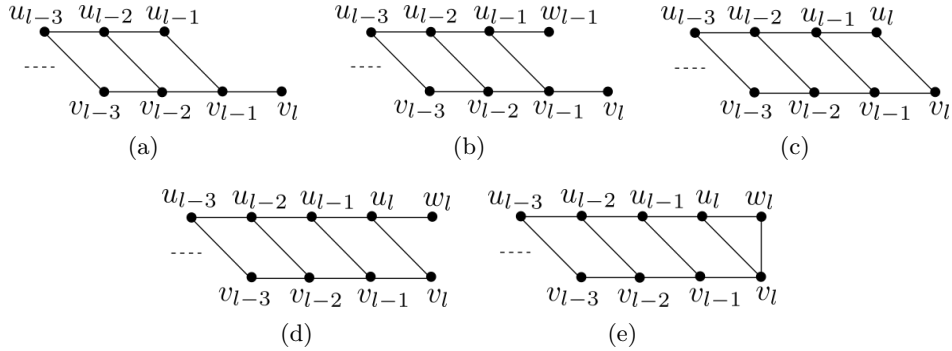


FIGURE 40

Case (ii): $k = 3$. G has a subgraph (a) of the following figure. The left side of G must be (a) or (b) of the following figure and all possible forms of the right side have been shown in Figure 40.

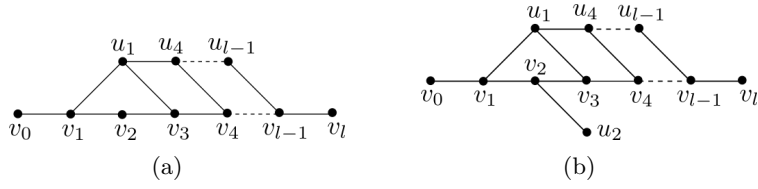


FIGURE 41

Case (iii): $4 \leq k \leq l - 2$. G has a subgraph shown in the following figure which is the same with case (ii) by switching u_{i-2} and v_{i-1} , $4 \leq i \leq k$.

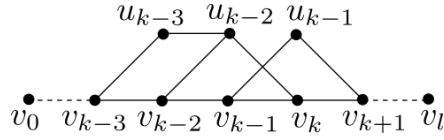


FIGURE 42

Case (iv): $j = l - 1$. G contains a subgraph shown in the following figure which is the same with (a) of Figure 41 if $u_{l-2} \sim v_l$, or (b) of Figure 41 if $u_{l-2} \approx v_l$ as $P' = v_l v_{l-1} \cdots v_0$ is also a diameter.

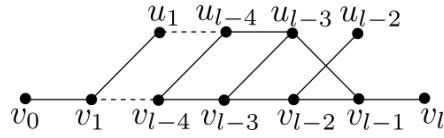


FIGURE 43

By previous discussions, we prove that if G is not a prism graph or a Möbius ladder, then it has one of the following forms, which are isometric to graphs in Figure 45.

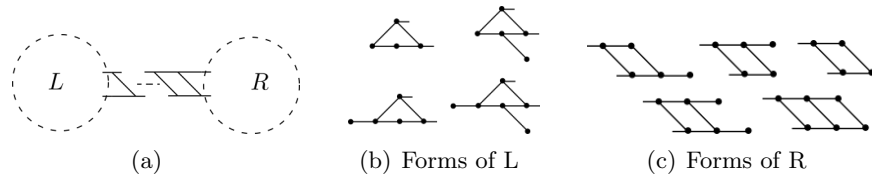


FIGURE 44

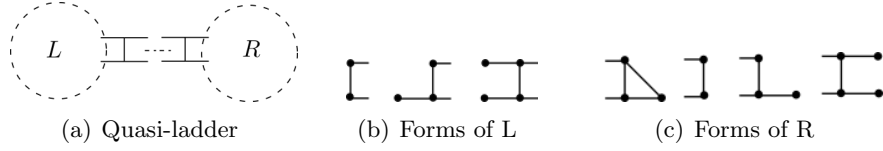


FIGURE 45

□

Theorem 4.7. Let $P = v_0v_1 \cdots v_l$, $l \geq 6$, be a diameter of $G \in \mathcal{G}$. Suppose that for all $1 \leq i \leq l-1$, $s(v_i) \neq 3^0$, $s(v_i) \neq 3^-$, and there exists $s(v_i) = 3^+$, then G is a prism graph, a Möbius ladder or a quasi-ladder.

Proof. In fact we will prove that graphs considered in this theorem have been discussed in the previous theorems. Let $k = \max\{i : 1 \leq i \leq l-1, s(v_i) = 3^+\}$, then $k = l-2$ or $l-1$.

Case (i): $k = l-2$. Then $\deg(v_{l-1}) = 2$ and G has a subgraph shown in figure (a). By applying local structure $(3^+, 2)$ on $v_{l-3}v_{l-2}v_{l-1}v_l$, we get that G has a subgraph (b) or (c). We have discussed those graphs by changing $P = v_0v_1 \cdots v_l$ to $P' = v_lv_{l-1} \cdots v_0$.

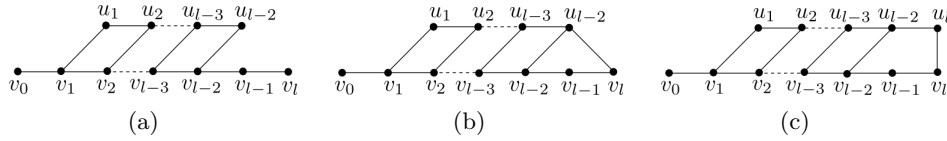


FIGURE 46

Case (ii): $k = l-1$. G contains one of the followings as a subgraph, which have been discussed in the previous theorems by changing $P = v_0v_1 \cdots v_l$ to $P' = v_lv_{l-1} \cdots v_0$.

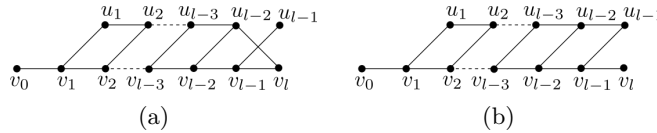


FIGURE 47

□

Now, we give the proofs of Theorem 1.1 and 1.2.

Proof of Theorem 1.1. By applying Theorem 4.3, 4.5, 4.6 and 4.7, we obtain the conclusion. □

Proof of Theorem 1.2. As G is an infinite graph, we can find an infinite geodesic path P which is isometric to \mathbb{Z} or \mathbb{Z}^+ . By applying the arguments used for finite graphs, we get the conclusion. \square

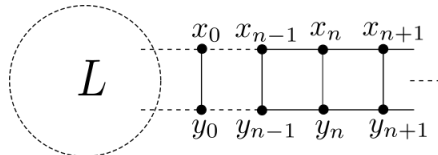
5. APPLICATIONS

In this section, as an application of the main results, we establish the following strong Liouville property.

Theorem 5.1. *Let $G \in \mathcal{G}$ be an infinite graph, then all positive harmonic functions on G are constant.*

Proof. By Theorem 1.2, G is a line, half line, infinite ladder or infinite quasi-ladder. As line and infinite ladder are finitely generated Cayley graphs of Abelian groups, all positive harmonic functions on them are constant; see [CD60]. Besides, Hua and Münch also proved all positive harmonic functions are constant on graphs with two ends and nonnegative Ricci curvature, which provides another proof for the strong Liouville property of line and infinite ladder; see [HM21, Theorem 5.9]. For a half line, there is a stronger conclusion. In fact all harmonic functions on a half line are constant. So, we only consider the quasi-ladder case.

Let f be a positive harmonic function on G . If f is not a constant, there exist $i \geq 0$, such that $f(x_i) \neq f(y_i)$. Without loss of generality, we assume $i = 0$. By choosing suitable constants a and b such that $g := af + b$ satisfies $g(x_0) = 1$ and $g(y_0) = 0$, we get a harmonic function g which is bounded from below or above.



For any $n \in \mathbb{Z}^+$, we have

$$g(x_n) = \frac{1}{3}(g(x_{n-1}) + g(x_{n+1}) + g(y_n)),$$

$$g(y_n) = \frac{1}{3}(g(y_{n-1}) + g(y_{n+1}) + g(x_n)).$$

Let $z_n = g(x_n) - g(y_n)$, $h_n = g(x_n) + g(y_n)$. We have $4z_n = z_{n-1} + z_{n+1}$, $2h_n = h_{n-1} + h_{n+1}$. On the one hand, it is easy to check that $h_n = O(n)$. On the other hand, $z_n \geq z_{n-1}$ by the maximum principle. Thus $z_{n+1} \geq 3z_n$, which means that $z_n \geq C \cdot 3^n$ for some constant $C > 0$. It follows that $g(y_n) \rightarrow -\infty$ and $g(x_n) \rightarrow +\infty$ as $n \rightarrow +\infty$. We get a contradiction as g is bounded from below or above. \square

ACKNOWLEDGMENTS

The authors are grateful to Prof. Bobo Hua for his guidance and support. The authors would also like to thank Florentin Münch and David Cushing for their helpful advice.

REFERENCES

- [BCL⁺18] D. P. Bourne, D. Cushing, S. Liu, F. Münch, and N. Peyerimhoff. Ollivier-Ricci idleness functions of graphs. *SIAM J. Discrete Math.*, 32(2):1408–1424, 2018.
- [BHL⁺15] Frank Bauer, Paul Horn, Yong Lin, Gabor Lippner, Dan Mangoubi, and Shing-Tung Yau. Li-Yau inequality on graphs. *J. Differential Geom.*, 99(3):359–405, 2015.
- [BHLY20] Shuliang Bai, An Huang, Linyuan Lu, and Shing-Tung Yau. On the sum of ricci-curvatures for weighted graphs. *arXiv preprint arXiv:2001.01776*, 2020.
- [BLY21] Shuliang Bai, Linyuan Lu, and Shing-Tung Yau. Ricci-flat graphs with maximum degree at most 4. *arXiv preprint arXiv:2103.00941*, 2021.
- [CD60] Gustave Choquet and Jacques Deny. Sur l'équation de convolution $\mu = \mu * \sigma$. *C. R. Acad. Sci. Paris*, 250:799–801, 1960.
- [CG72] Jeff Cheeger and Detlef Gromoll. The splitting theorem for manifolds of non-negative Ricci curvature. *J. Differential Geometry*, 6:119–128, 1971/72.
- [CKL⁺18] David Cushing, Riikka Kangaslampi, Yong Lin, Shiping Liu, Linyuan Lu, and Shing-Tung Yau. Ricci-flat cubic graphs with girth five. *arXiv preprint arXiv:1802.02982*, 2018.
- [CKL⁺19] David Cushing, Riikka Kangaslampi, Valtteri Lipiäinen, Shiping Liu, and George W Stagg. The graph curvature calculator and the curvatures of cubic graphs. *Experimental Mathematics*, pages 1–13, 2019.
- [CP18] Hee Je Cho and Seong-Hun Paeng. Classification of α -Ricci flat graphs with girth at least five. *Discrete Math.*, 341(10):2894–2902, 2018.
- [HLLY19] Paul Horn, Yong Lin, Shuang Liu, and Shing-Tung Yau. Volume doubling, Poincaré inequality and Gaussian heat kernel estimate for non-negatively curved graphs. *J. Reine Angew. Math.*, 757:89–130, 2019.
- [HLYY18] Weihua He, Jun Luo, Chao Yang, and Wei Yuan. Ricci-flat graphs with girth four. *arXiv preprint arXiv:1807.07253*, 2018.
- [HM21] Bobo Hua and Florentin Münch. Every salami has two ends. *arXiv preprint arXiv:2105.11887*, 2021.
- [Hua19] Bobo Hua. Liouville theorem for bounded harmonic functions on manifolds and graphs satisfying non-negative curvature dimension condition. *Calc. Var. Partial Differential Equations*, 58(2):Paper No. 42, 8, 2019.
- [JMR19] Jürgen Jost, Florentin Münch, and Christian Rose. Liouville property and non-negative ollivier curvature on graphs. *arXiv preprint arXiv:1903.10796*, 2019.
- [LLY11] Yong Lin, Linyuan Lu, and Shing-Tung Yau. Ricci curvature of graphs. *Tohoku Math. J. (2)*, 63(4):605–627, 2011.
- [LLY14] Yong Lin, Linyuan Lu, and S.-T. Yau. Ricci-flat graphs with girth at least five. *Comm. Anal. Geom.*, 22(4):671–687, 2014.
- [LY10] Yong Lin and Shing-Tung Yau. Ricci curvature and eigenvalue estimate on locally finite graphs. *Math. Res. Lett.*, 17(2):343–356, 2010.
- [MW19] Florentin Münch and Radosław K. Wojciechowski. Ollivier Ricci curvature for general graph Laplacians: heat equation, Laplacian comparison, non-explosion and diameter bounds. *Adv. Math.*, 356:106759, 45, 2019.
- [Oll07] Yann Ollivier. Ricci curvature of metric spaces. *C. R. Math. Acad. Sci. Paris*, 345(11):643–646, 2007.

- [Oll09] Yann Ollivier. Ricci curvature of Markov chains on metric spaces. *J. Funct. Anal.*, 256(3):810–864, 2009.
- [Sch99] Michael Schmuckenschläger. Curvature of nonlocal Markov generators. In *Convex geometric analysis (Berkeley, CA, 1996)*, volume 34 of *Math. Sci. Res. Inst. Publ.*, pages 189–197. Cambridge Univ. Press, Cambridge, 1999.
- [Yau75] Shing Tung Yau. Harmonic functions on complete Riemannian manifolds. *Comm. Pure Appl. Math.*, 28:201–228, 1975.

FENGWEN, HAN: SCHOOL OF MATHEMATICAL SCIENCES, FUDAN UNIVERSITY, SHANGHAI 200433, CHINA

Email address: `fwhan19@fudan.edu.cn`

TAO, WANG: SCHOOL OF MATHEMATICAL SCIENCES, FUDAN UNIVERSITY, SHANGHAI 200433, CHINA

Email address: `taowang21@m.fudan.edu.cn`